Published in final edited form as:
Neuron. 2014 July 16; 83(2): 361–371. doi:10.1016/j.neuron.2014.06.030.

ABHD6 blockade exerts antiepileptic activity in PTZ-induced seizures and in spontaneous seizures in R6/2 mice

Alipi V. Naydenov[#1,2], **Eric A. Horne**[#3], **Christine S. Cheah**[3], **Katie Swinney**[3], **Ku-Lung Hsu**[4], **Jessica K. Cao**[3], **William Marrs**[2], **Jacqueline L. Blankman**[4], **Sarah Tu**[3], **Allison E. Cherry**[3], **Susan Fung**[2], **Andy Wen**[5], **Weiwei Li**[4], **Michael S. Saporito**[6], **Dana E. Selley**[7], **Benjamin F. Cravatt**[4], **John C. Oakley**[3,8], and **Nephi Stella**[3,9]

[1]Medical Scientist Training Program, University of Washington, Seattle Washington, 98195, USA

[2]Neurobiology and Behavior Graduate Program, University of Washington, Seattle, Washington, 98195, USA

[3]Department of Pharmacology, University of Washington, Seattle, Washington, 98195, USA

[4]The Skaggs Institute for Chemical Biology and Department of Chemical Physiology, The Scripps Research Institute, La Jolla, California, 92037, USA

[5]Department of Biology, University of Washington, Seattle, Washington, 98195, USA

[6]Melior Discovery, Inc., Exton, Pennsylvania, 19341, USA

[7]Department of Pharmacology and Toxicology, Virginia Commonwealth University, Richmond, Virginia, 23298, USA

[8]Department of Neurology, University of Washington, Seattle, Washington, 98195, USA

[9]Department of Psychiatry and Behavioral Sciences, University of Washington, Seattle, Washington, 98195 USA

[#] These authors contributed equally to this work.

Abstract

The serine hydrolase α/β-hydrolase domain 6 (ABHD6) hydrolyzes the most abundant endocannabinoid (eCB) in the brain, 2-arachidonoylglycerol (2-AG), and controls its availability at cannabinoid receptors. We show that ABHD6 inhibition decreases pentylenetetrazole (PTZ)-

Corresponding Author: Nephi Stella, University of Washington, Department of Pharmacology, 1959 N.E. Pacific St., BB-1538, HSC Box 357280, Seattle WA, 98195 nstella@uw.edu.

Author contributions: AN, KS, and JC performed PTZ studies. CC and JO performed surgeries, and JO designed EEG studies and analyzed the data. AN and KS performed the histology. EH, KS, WM, AN, AC, SF, and AW carried out the R6/2 seizure studies. AN, WM and ST performed behavioral testing. KH and JB performed ABPP experiments, and WL and BC generated and provided the WWL123 compound. DS performed GTPγS assays, and MS performed pharmacokinetic studies. AN, EH, and NS designed the studies, and analyzed the data. AN and NS wrote the manuscript.

Conflict of Interest: The authors report no conflict of interest.

induced generalized tonic-clonic and myoclonic seizure incidence, and severity. This effect is retained in *cnr1*$^{-/-}$ or *cnr2*$^{-/-}$ mice, but blocked by addition of a subconvulsive dose of picrotoxin, suggesting the involvement of $GABA_A$ receptors. ABHD6 inhibition also blocked spontaneous seizures in R6/2 mice, a genetic model of Juvenile Huntington's disease known to exhibit dysregulated eCB signaling. ABHD6 blockade retained its antiepileptic activity over chronic dosing and was not associated with psychomotor or cognitive effects. While the etiology of seizures in R6/2 mice remains unsolved, involvement of the hippocampus is suggested by interictal epileptic discharges, increased expression of vGLUT1 but not vGAT, and reduced Neuropeptide Y (NPY) expression. We conclude that ABHD6 inhibition may represent a novel antiepileptic strategy.

Introduction

In the brain, a major role of the eCB signaling system is to control presynaptic neurotransmitter release (Di Marzo, 2011; Katona and Freund, 2012). This system comprises the CB_1 and CB_2 receptors and two main eCBs, anandamide and 2-AG, which are produced and inactivated by distinct lipases and hydrolases, respectively. We recently demonstrated that the serine hydrolase ABHD6 is a *bona fide* member of the eCB signaling system that controls the availability of 2-AG, but not anandamide, at CB_1 receptors (Marrs et al., 2011; 2010). Unlike other neurotransmitters which are synthesized and stored in synaptic vesicles for release, eCBs are produced on-demand in response to synaptic activity (Di Marzo et al., 1994; Stella and Piomelli, 2001a; Stella et al., 1997). In neurons, ABHD6 is located post-synaptically, at the site of 2-AG synthesis, where it fine-tunes the stimulated production of 2-AG and the resulting activation of presynaptic CB_1 cannabinoid receptors (Marrs et al., 2011; 2010). Because they rely on stimulated production of 2-AG, ABHD6 inhibitors augment 2-AG availability with spatiotemporal selectivity (Ahn et al., 2008; Blankman et al., 2007; Marrs et al., 2010). Therefore, this enzyme represents a possible molecular hub that controls the 2-AG/CB_1 arm of eCB signaling (Stella, 2012). Recent studies suggest that 2-AG may also act at $GABA_A$ receptors (Baur et al., 2013; Sigel et al., 2011), and since both $GABA_A$ and ABHD6 are located post-synaptically, the availability of 2-AG at $GABA_A$ receptors might be regulated by ABHD6 activity.

Epilepsy is a common condition that is refractory to current therapies in approximately 30% of patients and is associated with pathologic cortical excitability (Kwan and Brodie, 2000). Current anti-epileptic drugs target voltage-gated ion channels to reduce neuronal excitability either directly or *via* modulation of synaptic transmission. However, the therapeutic benefit of these treatments is limited by a lack of efficacy in some patients, as well as by their side effect profiles, underlining the need for developing new pharmacological strategies for the treatment of epilepsy. Targeting neuromodulatory signaling systems (like eCB signaling) that control endogenous homeostatic mechanisms in a state-dependent manner may provide greater efficacy and tolerability. Evidence shows that synthetic agonists at CB_1 receptors reduce glutamatergic synaptic activity and protect rodents against chemically-induced seizures (Chen et al., 2007; Lafourcade et al., 2007; Marsicano, 2003; Rudenko et al., 2012), although paradoxical mechanisms whereby eCBs have pro-convulsant effects have also been described (Clement et al., 2003). Inhibitors of eCB hydrolysis retain the ability to reduce

glutamatergic synaptic activity, but unlike CB_1 receptor agonists, these inhibitors rely on stimulated production of ligand (eCBs) and thus selectively augment CB_1 signaling at active synapses. Among eCB hydrolases, ABHD6 is unique because its postsynaptic location allows for the control of 2-AG availability despite its low intrinsic activity compared to monoacylglycerol lipase (MGL), the primary brain 2-AG hydrolase that controls the bulk of 2-AG levels (Blankman et al., 2007; Marrs et al., 2010). Thus, whereas MGL controls 2-AG levels at presynaptic terminals, ABHD6 fine-tunes the activity dependent production of 2-AG at active synapses.

We hypothesized that ABHD6 blockade by WWL123, a brain penetrant selective inhibitor, would protect against PTZ-induced epileptiform seizures without resulting in overt psychomotor effects. Chemically-induced seizure models represent a typical initial drug-screening platform and provide predictive power for the discovery of anti-epileptic drugs (White, 2003). However, this approach may miss compounds that could be effective against specific epilepsies, including therapy-resistant seizures, and have the drawback of inducing seizures in otherwise healthy mice (Bialer and White, 2010; Smith et al., 2007). Based on this rationale, we sought to test the ability of ABHD6 blockade to control seizures in a genetic seizure model known to be associated with impaired eCB signaling. Specifically, R6/2 mice display both spontaneous and audiogenic seizures (Cepeda-Prado et al., 2012; Mangiarini et al., 1996) and reproduce the profound dysregulation of eCB signaling described in Huntington's disease (HD) patients (Bisogno et al., 2008; Centonze et al., 2005). R6/2 mice have both decreased 2-AG availability (Bisogno et al., 2008) and CB_1 receptor down-regulation in select neuronal populations (Dowie et al., 2009; Glass et al., 2000; 1993; Horne et al., 2012). Here too, we hypothesized that ABHD6 inhibition would prevent spontaneous seizures in R6/2 mice by augmenting 2-AG signaling.

Results

Pharmacokinetic profile and target engagement of WWL123 and SR141716

To study the role of *in vivo* ABHD6 blockade in seizure incidence, we first validated our pharmacological approach. WWL123 is a carbamate (Figure S1A) which was discovered in a screen of 70+ serine hydrolases as a specific inhibitor of ABHD6 (IC_{50} = 0.43μM), and *in vivo* dose-response studies identified 10 mg/kg as an optimal treatment dose (Bachovchin et al., 2010). To confirm these findings, we dosed C57BL/6 mice with vehicle or WWL123 (10 mg/kg, i.p.) and four hours later prepared homogenized cortical samples for activity-based protein profiling (ABPP) to verify that WWL123 crosses the blood-brain-barrier and inhibits ABHD6 in brain parenchyma. We found that this treatment reduced ABHD6 labeling by the FP-rhodamine and the HT-01 probe (Hsu et al., 2012; 2013a; 2013b), both of which label serine hydrolases in an activity-dependent manner (Figure S1B-C). Importantly, WWL123 treatment did not affect the labeling of other serine hydrolases, such as fatty acid amide hydrolase (FAAH) and monoacylglycerol lipase (MGL), further validating the selectivity of this inhibitor for ABHD6.

Similarly, we studied the pharmacokinetic profile of the CB_1 antagonist SR141716 (SR1) and found that subcutaneous (s.c.) injection results in sustained accumulation of the compound in brain parenchyma, resulting in the largest total drug exposure (6272

ng*hr/mL) compared to other routes of administration. Notably, s.c. SR1 reached a peak brain concentration of 180 ± 100 nM (C_{max}) 2 hours following s.c. injection and remained above 100 nM for several hours, providing a wide and reliable window for experimental manipulation (Figure S1D-E, Table S1). We confirmed the functional blockade of CB_1 signaling by harvesting cortical brain tissue from mice treated with this regimen and measuring CB_1 receptor activity by GTPγS assays (Figure S1F; vehicle, EC_{50} = 8.9 ± 1.6 nM; SR1, EC_{50} = 26.0 ± 2.8 nM; t=5.481, df = 8, p = 0.001). These results identify s.c. treatment with 10 mg/kg SR1 and i.p. treatment with 10 mg/kg WWL123 as optimal for CB_1 receptor antagonism and ABHD6 inhibition in mice, respectively.

ABHD6 blockade reduces PTZ-induced seizures

PTZ induces epileptiform seizures in healthy mice, typified by progression through increasingly severe stages of seizure leading to death in a subset of individuals. Mice were pretreated with either vehicle or 10 mg/kg WWL123, treated with 50 mg/kg PTZ and behavioral seizures captured by video recording. PTZ induced seizures that progressed from hypoactivity (stage 1), to partial clonus (stage 2), to generalized clonus (stage 3), culminated in global tonic-clonic (GTC) seizures (stage 4), and were associated with death in 11% of cases. Pretreatment with WWL123 blocked seizure-related mortality, reduced the severity of seizure behaviors (Figure 1A), reduced the number of GTC seizures *per* mouse (from 1.90 ± 0.28 to 0.60 ± 0.22, Figure 1B), and also reduced the frequency of myoclonic (MC) seizures (11.05 ± 0.51 to 7.29 ± 0.84, Figure 1C). Note that ABHD6 blockade is not effective against stronger seizures induced by 70 mg/kg PTZ (Figure S2A-D) or in a status-epilepticus-like state induced by 30 mg/kg kainate (Figure S2E-F).

To measure the electrographic changes between PTZ-treated mice and PTZ+WWL123 treated mice, we recorded electrocorticograms (ECoG) with bilateral epidural screw electrodes (see methods) in the following brain areas: primary somatosensory cortex (ECoG), cortical local field potentials in layer V frontal cortex (LFP_{CTX}) and hippocampal local field potential in CA1 (LFP_{HIP}) with fine-wire depth electrodes referenced to a screw electrode over the olfactory bulb. Two days after recovery from surgery, the mice were administered PTZ, either with or without a 4 hours pretreatment with WWL123. Both mice receiving PTZ and mice receiving PTZ+WWL123 experienced a GTC episode (with behaviors corresponding to stage 4) within the first 10 min after PTZ administration, with epileptiform activity evolving in all channels simultaneously out of background EEG. Similarly, both groups experienced myoclonic seizures accompanied by behavioral myoclonus that preceded the GTC episode, however the group pretreated with WWL123 had fewer myoclonic seizures (Figure 1D-E). We conclude that WWL123 reduces the frequency and severity of PTZ-induced seizures and protects against seizure-related death. Video-EEG monitoring confirmed that electrographic features of PTZ-induced seizures were similar between treatments, and that no electrographic seizures without behavioral correlates were seen in either group. Therefore, to minimize the confounding effect of surgery, further studies were performed using behavioral observation.

The anticonvulsive effects of WWL123 involve $GABA_A$ and not CB_1 or CB_2 receptors

To test the hypothesis that the antiepileptic effect of WWL123 is due to increased CB_1 signaling, we tested the effect of WWL123 on PTZ-induced seizures in WT and *cnr1*$^{-/-}$ mice. The protective effect of ABHD6 blockade was retained in *cnr1*$^{-/-}$ mice (Figure 2A) across measures of seizure susceptibility, number of GTCs, and number of MCs, without interaction between genotype and treatment (see Table S3 for full statistical testing results). To rule out the involvement of CB_2 receptors, we tested WWL123 on PTZ-induced seizures in *cnr2*$^{-/-}$ mice. Similar to what we observed in *cnr1*$^{-/-}$ mice, the protective effect of WWL123 on seizure susceptibility and MC was preserved in *cnr2*$^{-/-}$ mice (Figure 2B), without interaction between genotype and treatment, but in this experiment WWL123 did not reduce GTCs in either WT or *cnr2*$^{-/-}$ mice (Table S3). It was our observation that GTCs were generally the most variable measure between separate experiments. We conclude that the protective effect of ABHD6 blockade is independent of CB_1 and CB_2 receptors.

Recent reports have described a direct interaction between 2-AG and the $GABA_A$ receptor (Baur et al., 2013; Sigel et al., 2011), therefore we tested whether $GABA_A$ receptors are required for the anticonvulsive effect of ABHD6 blockade by co-treating with WWL123 and the $GABA_A$ antagonist picrotoxin. Using a dose of 1 mg/kg picrotoxin, below the dose range (>5mg/kg) required to produce seizures on a single dosing (Nutt et al., 1982), animals were treated with WWL123 or vehicle (4 hours prior to receiving PTZ), and then with picrotoxin (1 mg/kg, i.p.) or vehicle (5 minutes prior to receiving PTZ). As expected, picrotoxin did not exacerbate PTZ-induced seizures (Figure 2C); however when $GABA_A$ receptors were blocked by picrotoxin, WWL123 no longer reduced seizure susceptibility, GTCs, and MC. Statistical analysis of these results indicate an interaction effect between picrotoxin and WWL123 in both seizure susceptibility and MC, and a trend in GTCs (Table S3). This result suggests that the anticonvulsant quality of ABHD6 inhibition in PTZ-induced epileptiform seizures is likely mediated through $GABA_A$ receptors (see model in Figure 2D).

R6/2 mice experience electrographic and behavioral seizures

R6/2 mice are known to experience both spontaneous and audiogenic seizures (Cepeda-Prado et al., 2012; Mangiarini et al., 1996), yet neither qualitative nor quantitative analysis of spontaneous seizures or of the possible etiology of these seizures is available. To determine how electrographic features of seizures correlate with observed behaviors, we performed EEG recordings in tandem with video recording. ECoGs were recorded with screw electrodes placed bilaterally over frontal cortex, and LFPs were recorded with fine-wire depth electrodes placed bilaterally superficial to CA1, referenced to a screw electrode over the olfactory bulb. Animals were given 5-7 days to recover after surgeries and were then monitored on two consecutive days for 6 hours intervals. Spontaneous seizures were captured in this manner in three separate R6/2 mice. Figure 3A shows a representative example of an EEG accompanying a spontaneous behavioral seizure. The electrographic and behavioral onsets of the seizure were closely time-locked, seizure behaviors persisted throughout the entire electrographic seizure, and after the seizure there was both postictal suppression on the EEG and a behavioral pause (Figure 3B). Furthermore, similar behavioral findings were observed in mice with and without surgical procedures, indicating

that surgeries did not change the nature of the seizures in R6/2 mice, thus further studies were performed using behavioral observation (see discussion in methods).

Electrographic and histological abnormalities in R6/2 hippocampus

LFP recordings from hippocampi (Figure 4A-C) revealed interictal epileptic discharges in R6/2 but not WT mice, consisting of high amplitude (>3mV), sharply contoured complexes which transiently disrupted ongoing hippocampal activity (suppression), and were associated with high frequency oscillations (fast ripples), two criteria for hippocampal epileptic discharge (Bragin et al., 1999; Engel et al., 2009). We reviewed EEG for epileptic activity, which we defined as sharply contoured spikes that deviated by more than three standard deviations from root-mean-square (rms) of background activity. Unlike our findings in hippocampus, we did not find epileptic activity in cortical leads except in association with larger hippocampal spikes. Epileptic complexes were not seen in recordings of WT mice. Interictal spikes are associated with network hyperexcitability and are consistent with an increased risk of partial-onset seizures.

We stained for anatomical indices of synaptic excitability in hippocampal areas CA1, CA2, and CA3 and found increased vGlut1 expression in R6/2 mice compared to wild-type mice (one way ANOVA, CA1: p=0.02; CA2: p=<0.001; CA3 p=0.004), while vGAT expression remained unchanged (Figures 4D-F). The imbalance of these markers suggests increased excitability without a corresponding increase in inhibitory tone. While disturbances in the eCB system have been well described in the striatum and cortex of R6/2 mice, the state of eCB system in the hippocampus of this mouse line has not been reported. We found a small increase in ABHD6 immunoreactivity in the CA1 and CA2 regions of R6/2 mice compared to wild-type mice (Figure S3A-B), whereas CB_1 was decreased specifically in vGlut1-positive pixels, suggesting a selective decrease in glutamatergic terminals (Figure S3C-F). NPY inhibits excitatory neurotransmission (Colmers et al., 1988), by synapsing onto presynaptic mossy fiber (CA2/CA3) and Schaffer collateral (CA1) terminals (Baraban et al., 1997), and exerts powerful anticonvulsant effects through Y5 receptors (Marsh et al., 1999; Vezzani et al., 1999; Woldbye et al., 1997). Deletion of *npy* has been associated with temporal seizures (Baraban et al., 1997; Erickson et al., 1996) that are blocked by both intraventricular administration of NPY (Woldbye et al., 1996) and NPY gene therapy (Noe et al., 2008). We measured a profound reduction in NPY immunoreactivity in the hippocampus of R6/2 mice, compared with wild type, (p=0.004) (Figure 4G, and Figure S4), suggesting a candidate mechanism (Figure 4H) for epileptogenesis in R6/2 mice. Together, these findings support our strategy to test the utility of ABHD6 blockade in a genetic model of seizures featuring electrographic and histological abnormalities in hippocampus.

ABHD6 inhibitor blocks behavioral seizures in R6/2 mice in a CB_1-independent manner

To test whether behavioral seizures exhibited by R6/2 mice are controlled by chronic pharmacological blockade of the ABHD6/CB_1 arm of the eCB signaling system, we treated these mice with a daily injection of either vehicle, SR1 or WWL123 beginning at 4 weeks of age (Figure 5A). Note that we did not observe overt side effects associated with chronic WWL123 administration during the 8 weeks of treatment period and did not observe any sign of psychomotor impairment, as measured by open field (Figure S5A), novel object

recognition (Figure S5B-C) and elevated plus maze (Figure S5D-E). We found that SR1 increased, and WWL123 blocked, the incidence of spontaneous behavioral seizures in R6/2 mice (Figure 5B-C; Vehicle=31%, SR1=80%, WWL123=0%; 2x3 contingency table analyzed by Fisher's Exact Test, p=0.023). There was no effect (Veh = 64.4 ± 7.5s; SR1 = 60.3 ± 20.1s, p=0.89) on duration of spontaneous seizures in response to chronic SR1 treatment (Veh = 64.4 ± 7.5s; SR1 = 60.3 ± 20.1s, p=0.89). These results indicate that chronic ABHD6 inhibition is effective against spontaneous seizures in a genetic model of epilepsy and that no tolerance develops to prolonged treatment with WWL123. The involvement of $GABA_A$ receptors could not be tested in R6/2 mice because chronic low-dose GABA antagonists result in kindling in WT mice (White, 2003).

To assess the mechanism of antiepileptic action of ABHD6 blockade in R6/2 mice, we acutely treated 9-week-old drug-naïve mice with a single injection of either vehicle, SR1, WWL123, or SR1+WWL123, and monitored the animals for six hours with video recording (Figure 5D-E). Videos were scored for behavioral seizures of Racine grade 4-6. Similar to what we observed with chronic treatment, acute treatment with WWL123 prevented seizures and acute treatment with SR1 increased the number of seizures observed over 6 hours. However, SR1 treatment did not antagonize the effect of WWL123, suggesting the absence of CB_1 receptor-involvement in the protective effect of WWL123 (Vehicle=8%, SR1=63%, WWL123=0%, SR1+WWL123=0%; 2x4 contingency table analyzed by Fisher's Exact Test, p=0.006). Here too, the involvement of $GABA_A$ receptors could not be tested with picrotoxin because of its short duration of action compared with WWL123 or SR1, and because of the long observation window needed to reliably capture spontaneous seizures. Together with results obtained in the PTZ-induced seizure model, this result suggests that the antiepileptic activity of ABHD6 inhibition operates through a CB_1-independent mechanism.

Discussion

ABHD6 is a newly identified member of the eCB signaling system responsible for controlling the post-synaptic production of 2-AG (Marrs et al., 2010). We now show that ABHD6 blockade by WWL123 exerts an antiepileptic effect in PTZ-induced epileptiform seizures and spontaneous seizures in R6/2 mice. We found that the antiepileptic activity of ABHD6 blockade against PTZ-induced seizures is independent of both CB_1 and CB_2 receptors, and likely dependent on $GABA_A$ receptors. A direct and positive allosteric modulation of $GABA_A$ receptors by 2-AG has been demonstrated (Sigel et al., 2011), and subsequent molecular modeling paired with site-directed mutagenesis identified the inner (cytosolic) leaflet of the β2 subunit of $GABA_A$ as the binding site for 2-AG (Baur et al., 2013). Based on this evidence, post-synaptic production of 2-AG could signal through $GABA_A$ receptors in an autocrine manner, and the postsynaptic localization of ABHD6 places this enzyme in an ideal location to control the availability of 2-AG at $GABA_A$ receptors. Note that we also cannot exclude the possibility that the antiepileptic effect of ABHD6 blockade is mediated by a molecular species besides 2-AG, as ABHD6 has other known substrates (Navia-Paldanius et al., 2012; Thomas et al., 2013). Also note that an indirect effect of 2-AG on $GABA_A$ mediated through CB_1 receptors is unlikely because CB_1

activity decreases GABA release (Wilson and Nicoll, 2001) and because the antiepileptic effect of WWL123 is not lost in *cnr1*$^{-/-}$ mice or after treatment with SR1.

There are major drawbacks to currently available therapeutic approaches for the treatment of epilepsy, including tolerance to the efficacy of antiepileptic drugs and increased likelihood of dose-related side effects, both of which reduce their clinical utility. When treating mice daily with WWL123 for 5 weeks, we did not observe tolerance to chronic ABHD6 blockade, in contrast to what is seen after chronic treatment with CB_1 receptor agonists and with MGL inhibitors (Blair et al., 2009; Schlosburg et al., 2010). Furthermore, we did not observe signs of motor or cognitive impairment typically associated with both CB_1 agonists and to a lesser degree with MGL inhibitors, nor did we observe sedation as is seen with $GABA_A$ agonists (van Rijnsoever, 2004). Lack of tolerance and the absence of measurable off-target behavioral effects might be due to the spatiotemporal specificity of ABHD6 blockade that is derived from a combination of the activity-dependence of 2-AG synthesis (Di Marzo, 2011; Stella and Piomelli, 2001b) and its weak enzymatic activity that controls only local levels of 2-AG (Marrs et al., 2011; 2010). Together, these findings suggest that ABHD6 inhibitors might exhibit a favorable safety profile and be amenable to long-term use for the treatment of seizures.

Among HD patients, individuals that carry more than 60 CAG repeats in the huntingtin gene begin exhibiting symptoms in their teens (or even younger as the number of repeats increases) (Andrew et al., 1993). This subset of patients are afflicted by Juvenile HD (JHD), an early and more aggressive variant of the disease which uniquely features myoclonic seizures in 38% of patients (Cloud et al., 2012), which are refractory to standard anti-epileptic medications (Osborne et al., 1982; Landau and Cannard, 2003; Gonzalez-Alegre and Afifi, 2006). Therefore epilepsy is emerging as a major co-morbidity and unmet medical need of patients with JHD and yet little is known about the molecular mechanisms underlying seizure incidence in this patient population. R6/2 mice recapitulate several aspects of an early-onset, rapidly progressive JHD phenotype, including both spontaneous seizures and early death (Bates and Woodman, 2009; Mangiarini et al., 1996). Here we show that behavioral seizures in R6/2 mice correspond to electrographic seizures and that ABHD6 blockade controls these seizures through a CB-independent mechanism. Our initial characterization of the seizures exhibited by R6/2 mice suggests hippocampal involvement. Interictal discharges with amplitude, morphology, and frequency components characteristic of epileptic discharges were observed in hippocampal leads. Since the purpose of the current study was to explore the anticonvulsive and antiepileptic efficacy of ABHD6 inhibition, follow-up studies are required. We note that our recordings do not rule out an epileptic focus outside of the hippocampus, and that recordings with higher spatial and temporal resolution are required, although this approach is technically challenging due to the hypersensitivity to anesthesia displayed by R6/2 mice and the fact that they experience anesthesia-related death with long surgery times (see methods). Additional, longer duration recordings with quantitative analysis are required to fully characterize the epileptic phenotype of R6/2 mice.

We observed a striking reduction of NPY expression throughout the hippocampus, and NPY deletion has been shown to result in temporal seizures that in turn can be rescued by intraventricular injection of exogenous NPY (Baraban et al., 1997; Erickson et al., 1996;

Woldbye et al., 1996). Reduced NPY in R6/2 mice is somewhat paradoxical, since seizure activity is typically associated with increases in hippocampal NPY expression (Vezzani et al., 1994). NPY interneurons provide presynaptic inhibition at mossy fibers (CA2/3) and at Shaffer collaterals (CA1), both of which are excitatory, and accordingly our results show increased expression of vGLUT1, but not vGAT, in CA1, CA2, and CA3 stratum pyramidale. Mutant huntingtin dysregulates the expression pattern of hundreds of genes (Luthi-Carter et al., 2002; 2000), including many members of the eCB family. Therefore, it is possible that mutant huntingtin decreases hippocampal NPY expression, which in turn results in a disinhibition of both Shaffer collaterals and mossy fibers. The resulting increased excitatory drive in the hippocampus could ultimately manifest as seizure activity.

In summary, this study identifies the recently described 2-AG hydrolase ABHD6 as a potential therapeutic target for epilepsy. To characterize the broader utility of this therapeutic strategy, it is necessary to outline the types of seizures that are sensitive to ABHD6 blockade. ABHD6 inhibitors should be systematically tested against classical models such as maximal electroshock, against acquired epilepsies such as traumatic brain injury (TBI)-induced seizures (White, 2003), as well as in models of treatment-resistant seizures such Dravet mice (Cheah et al., 2012; Kalume et al., 2013). Further experiments are needed to thoroughly demonstrate that ABHD6 inhibition proceeds directly through $GABA_A$ by increasing the local levels of 2-AG and its availability at $GABA_A$. Finally, given the superadditive $GABA_A$ responses induced by 2-AG and diazepam (Baur et al., 2013; Sigel et al., 2011), an isobolic study between these two drugs in an induced seizure paradigm would establish whether both therapeutic approaches could be used synergistically *in vivo* for antiepileptic therapy.

Experimental Procedures

Animals

All animal procedures were approved by the Institutional Animal Care and Use Committee for the University of Washington. For PTZ experiments, we used male C57Bl/6 mice. WT and *cnr1*$^{-/-}$ mice (Marsicano et al., 2002) were bred in our colony, and *cnr2*$^{-/-}$ mice (Deltagen) were gifted to us by Ken Mackie. Results obtained with animals treated with vehicle and WWL123 were generated using littermates within genotype. R6/2 mice present significant challenges for breeding, as all females and approximately half of males are sterile. Because these difficulties are compounded on a C57Bl/6 background, spontaneous behavioral seizure assays in R6/2 mice were performed on a mixed CBA-C57Bl/6 background in male and female littermates, and genders were balanced between cohorts. R6/2 (6-8 week old) males and wild type females (CBA-C57Bl/6) were bred to maintain the R6/2 colony (114 CAG repeats; sequenced at Laragen, Culver City, CA). Mice had *ad-libitum* access to food and water and were given additional wet food mash at 9 weeks of age. All R6/2 cages were provided with enrichment, and mice were not handled prior to experiments, other than to change cages or perform injections for chronic studies.

Drugs and Antibodies

SR141716 (SR1) was supplied by NIDA drug supply, WWL123 (WWL) was synthesized by the Cravatt Laboratory (Bachovchin et al., 2010), pharmasolve-n-methyl-2-pyrrolidone (Pharmasolve) was purchased from ISP Technologies (Columbia, MD), Cremophor RH40 and Lutrol F68 were purchased from BASF (Florham Park, NJ). Antibodies used for immunohistochemistry are listed in Table S2.

Drug pharmacokinetics and target validation

See supplemental methods for detailed description of pharmacokinetic, GTPγS, and affinity-based protein profiling (ABPP) procedures.

PTZ-induced seizures and monitoring

We performed i.p. injections of 50 or 70 mg/kg pentylenetetrazole (PTZ; Sigma, MO, USA) and then immediately placed animals in a 10”×18”×18” chamber with video recording (Zhang et al., 2010). Seizures were scored by two blinded observers according to a modified Racine scale designed specifically for PTZ-induced seizures in mice (Ferraro et al., 1999):

Stage 1: Hypoactivity culminating in behavioral arrest with contact between abdomen and the cage.

Stage 2: Partial clonus (PC) involving the face, head, or forelimbs.

Stage 3: Generalized clonus (GC) including all four limbs and tail, rearing, or falling.

Stage 4: Generalized Tonic-Clonic seizure (GTC)

Seizure susceptibility was calculated from the latencies to Stage 2-4, as previously described (Ferraro et al., 1999). Susceptibility scores are reported as a fraction of the average score for mice receiving only PTZ.

$$\text{Susceptibility score}=\Sigma\left(0.2*\frac{1}{\text{latency to PC}}+0.3*\frac{1}{\text{latency to GC}}+0.5*\frac{1}{\text{latency to GTC}}\right)$$

Myoclonic seizures (MC) and GTCs were also counted independently, because the seizure susceptibility score does not take into account the number of seizures. GTCs are reported as total number observed over 30 min after injection with PTZ. Because GTCs temporarily suppressed MCs, we counted MCs prior to the first GTC and reported them as MC/min, or in the case of animals that did not experience GTCs, we reported the rate of MCs over the first 10 min of the observation, in order to be comparable to animals that experienced GTCs.

Spontaneous Seizure Assays

Wild type and R6/2 mice were treated with 10 mg/kg SR1 (s.c.), 10 mg/kg WWL123 (i.p.), or vehicle (Pharmasolve:Cremophor RH40:1% Lutrol F68 [1:9:40]). Daily chronic treatment began at 4 weeks of age, one week after mice were weaned. Spontaneous seizure observations were conducted in 7-week-old (chronic) and 9-week-old (chronic and acute) R6/2 and wild type littermates. Mice were treated with SR1, WWL123, or SR1 + WWL123; SR1 was administered 90 min beforehand, and WWL123 was administered 120 min

beforehand. Following injection, mice were placed directly into a 10”×18”×18” plexiglass box and monitored for spontaneous behavioral seizures by video recording for 6 hours, then returned to their home cage. Behavioral seizures were scored from video recordings on the Racine scale (Racine, 1972) (1 = mouth and facial movement; 2 = head nodding; 3 = forelimb clonus; 4 = rearing with forelimb clonus; 5 = rearing and falling with forelimb clonus; 6 = tonic seizure followed by death). Videos were scored by at least two blinded observers who scored only behavioral seizures with Racine score of 4-6.

We noted a pronounced effect of the surgeries on the progressive phenotype of R6/2 mice. Specifically, only 54% of R6/2 mice survived ketamine/xylazine anesthesia, and overall, the genotype displayed hypersensitivity to anesthetics and required reduced dosing. For those that survived anesthesia, mice which did not have tremors or obvious motor impairment before the surgeries showed clear acceleration in phenotype after the surgeries with hunching, tremors, ataxia, and hypoactivity. In addition, the average survival of R6/2 mice was 1 week after surgery, which shortened their lifespan from the normal phenotype by at 2-4 weeks. Spontaneous seizures were not observed in the 72 hour window after surgery, suggesting a temporary effect of anesthesia on seizure incidence. Since our aim was to study spontaneous seizures which most accurately model the seizures occurring in juvenile HD patients, EEG surgeries were deemed confounding for accurate interpretation of our results and subsequent data was gathered by monitoring and grading behaviors without concomitant EEG. It should be noted that our monitoring protocol does not provide information on smaller seizures (Racine 1-3), or on electrographic seizures not resulting in seizure behaviors. Behaviors corresponding to Racine 1-3 were deliberately excluded because the authors felt that without concomitant EEG, which is not technically feasible due to the aggressive phenotype of the mice, scoring minor behaviors would lead to substantial error.

Semi-Quantitative Immunohistochemistry

Mice were euthanized 3 days after seizures and perfused with paraformaldehyde (4% in PBS), brains were extracted, post-fixed for 24 hrs, and cryoprotected in 15% sucrose (24 hrs) followed by 30% sucrose (48 hrs). Staining was performed as described in Horne *et al.* (Horne et al., 2012). Images were collected on a Leica SP1 Confocal Laser Scanning microscope with a 63x oil objective, and on an Olympus Fluoview-1000 Confocal microscope equipped with an automated stage and a 20x air or 63X oil objective. Images were analyzed using automated macros in a Fiji distribution of ImageJ (Schindelin et al., 2012). Thresholding was performed to remove background staining (threshold = mean+SD for all stains except NPY, threshold=mean+2*SD for NPY), and mean intensity of remaining pixels was calculated, a method we have previously validated (Horne et al., 2012).

Surgeries and Electroencephalograph (EEG) measurements

EEGs were performed as described by Oakley et al. (Oakley et al., 2009). Under ketamine/xylazine (130/8.8 mg/kg) anesthesia 6-8 week old mice were secured in a stereotactic headframe (David Kopf instruments) and using aseptic techniques a midline incision was made over the cranium before small burr holes were drilled for electrode placement bilaterally at 3 positions: LFP (A-P: +1.2mm; lateral: ± 3mm), EcoG (A-P: −0.7mm; lateral:

± 2.25mm), and Hippocampal (A-P: −2.02mm; lateral: ± 1.25mm). Higher impedance stainless steel fine wire electrodes (.003 inches uncoated, .0055 inches coated; A-M systems) were used for hippocampal and LFP depth electrodes and targeted to stratum radiatum of CA1 and layer V respectively. Lower impedance stainless steel screws (Amazon Supply) were used for ECoG recordings. Reference electrodes were placed over the olfactory bulb and ground was either a fully bared stainless steel fine wire or screw placed over the midline cerebellum. All electrodes were secured to the head with dental cement and connected to electrode interface boards (Neuralynx) for recording purposes, and placement was verified by Nissl stain. Animals were allowed to recover for one week following surgery. On the day of recordings, implanted mice were housed in a plexiglass box and EEG recordings were collected using a RZ2D bioamp processor (Tucker Davis Technologies) sampled at either 6 or 1.5 kHz and further analysis was conducted offline. Offline digital filtering was performed with Hamming-window based FIR filter for wideband (1-900 Hz), ripple (150-250 Hz), and fast ripple (300-600 Hz). Seizures were identified by characteristic sharp, rhythmic patterns consisting of repeated epileptic discharges followed by suppression of background activities. Simultaneous video recording was used to associate seizure behaviors with EEG patterns.

Data Analysis

Data were analyzed and graphed using PRISM 5 (GraphPad). All group tests for statistical significance in Figures 1-4 were performed using one-way ANOVA, except for interaction testing which was performed with two-way ANOVA. Post-hoc tests were analyzed by Fisher's T-Test. Contingency tables (Figure 5) were analyzed in R (http://cran.r-project.org), using Fisher's Exact test. Error bars depict standard error of the mean. EEG data were analyzed offline using Igor Pro 5.0 (Wavemetrics). Immunohistochemistry was analyzed using automated and unbiased macros written in the Fiji release of ImageJ (http://fiji.sc/Fiji).

Supplementary Material

Refer to Web version on PubMed Central for supplementary material.

Acknowledgments

We are grateful for helpful discussions with Franck Kalume and the University of Washington Statistical Consult Service. We also wish to acknowledge the contribution of the reviewers, who substantially improved the manuscript. *cnr2*$^{-/-}$ mice were kindly provided by Ken Mackie. Access to confocal microscopes provided by the Center for Human Disease and Disability Microscopy Center at the University of Washington (HD002274), and technical assistance was provided by Glen MacDonald. This study was funded by CHDI and NIH DA026430 (NS), DA033747 (AN), DA017259 (BC) and DA030404 (DS).

References

Ahn K, McKinney MK, Cravatt BF. Enzymatic pathways that regulate endocannabinoid signaling in the nervous system. Chem Rev. 2008; 108:1687–1707. [PubMed: 18429637]

Andrew SE, Paul Goldberg Y, Kremer B, Telenius H, Theilmann J, Adam S, Starr E, Squitieri F, Lin B, Kalchman MA, et al. The relationship between trinucleotide (CAG) repeat length and clinical features of Huntington's disease. Nat Genet. 1993; 4:398–403. [PubMed: 8401589]

Bachovchin DA, Ji T, Li W, Simon GM, Blankman JL, Adibekian A, Hoover H, Niessen S, Cravatt BF. Superfamily-wide portrait of serine hydrolase inhibition achieved by library-versus-library screening. Proc Natl Acad Sci USA. 2010; 107:20941–20946. [PubMed: 21084632]

Baraban SC, Hollopeter G, Erickson JC, Schwartzkroin PA, Palmiter RD. Knock-out mice reveal a critical antiepileptic role for neuropeptide Y. J. Neurosci. 1997; 17:8927–8936. [PubMed: 9364040]

Bates, GP.; Woodman, B. Juvenile Huntington's disease and mouse models of Huntington's disease. Oxford University Press; NY, USA: 2009.

Baur R, Kielar M, Richter L, Ernst M, Ecker GF, Sigel E. Molecular analysis of the site for 2-arachidonylglycerol (2-AG) on the β 2subunit of GABA Areceptors. J Neurochem. 2013; 126:29–36. [PubMed: 23600744]

Bialer M, White HS. Key factors in the discovery and development of new antiepileptic drugs. 2010:1–15.

Bisogno T, Martire A, Petrosino S, Popoli P, Di Marzo V. Symptom-related changes of endocannabinoid and palmitoylethanolamide levels in brain areas of R6/2 mice, a transgenic model of Huntington's disease. Neurochemistry International. 2008; 52:307–313. [PubMed: 17664017]

Blair RE, Deshpande LS, Sombati S, Elphick MR, Martin BR, DeLorenzo RJ. Prolonged exposure to WIN55,212-2 causes downregulation of the CB1 receptor and the development of tolerance to its anticonvulsant effects in the hippocampal neuronal culture model of acquired epilepsy. Neuropharmacology. 2009; 57:208–218. [PubMed: 19540252]

Blankman JL, Simon GM, Cravatt BF. A Comprehensive Profile of Brain Enzymes that Hydrolyze the Endocannabinoid 2-Arachidonoylglycerol. Chemistry & Biology. 2007; 14:1347–1356. [PubMed: 18096503]

Bragin A, Engel J, Wilson CL, Fried I, Mathern GW. Hippocampal and entorhinal cortex high-frequency oscillations (100--500 Hz) in human epileptic brain and in kainic acid--treated rats with chronic seizures. Epilepsia. 1999; 40:127–137. [PubMed: 9952257]

Centonze D, Rossi S, Prosperetti C, Tscherter A, Bernardi G, Maccarrone M, Calabresi P. Abnormal Sensitivity to Cannabinoid Receptor Stimulation Might Contribute to Altered Gamma-Aminobutyric Acid Transmission in the Striatum of R6/2 Huntington's Disease Mice. Biol. Psychiatry. 2005; 57:1583–1589. [PubMed: 15953496]

Cepeda-Prado E, Popp S, Khan U, Stefanov D, Rodriguez J, Menalled LB, Dow-Edwards D, Small SA, Moreno H. R6/2 Huntington's disease mice develop early and progressive abnormal brain metabolism and seizures. Journal of Neuroscience. 2012; 32:6456–6467. [PubMed: 22573668]

Cheah CS, Yu FH, Westenbroek RE, Kalume FK, Oakley JC, Potter GB, Rubenstein JL, Catterall WA. Specific deletion of NaV1.1 sodium channels in inhibitory interneurons causes seizures and premature death in a mouse model of Dravet syndrome. Proc Natl Acad Sci USA. 2012; 109:14646–14651. [PubMed: 22908258]

Chen K, Neu A, Howard AL, Földy C, Echegoyen J, Hilgenberg L, Smith M, Mackie K, Soltesz I. Prevention of Plasticity of Endocannabinoid Signaling Inhibits Persistent Limbic Hyperexcitability Caused by Developmental Seizures. Journal of Neuroscience. 2007; 27:46–58. [PubMed: 17202471]

Clement AB, Hawkins EG, Lichtman AH, Cravatt BF. Increased seizure susceptibility and proconvulsant activity of anandamide in mice lacking fatty acid amide hydrolase. J. Neurosci. 2003; 23:3916–3923. [PubMed: 12736361]

Cloud LJ, Rosenblatt A, Margolis RL, Ross CA, Pillai JA, Corey-Bloom J, Tully HM, Bird T, Panegyres PK, Nichter CA, et al. Seizures in juvenile Huntington's disease: Frequency and characterization in a multicenter cohort. Mov Disord. 2012; 27:1797–1800. [PubMed: 23124580]

Colmers WF, Lukowiak K, Pittman QJ. Neuropeptide Y action in the rat hippocampal slice: site and mechanism of presynaptic inhibition. J. Neurosci. 1988; 8:3827–3837. [PubMed: 2848110]

Di Marzo V. Endocannabinoid signaling in the brain: biosynthetic mechanisms in the limelight. Nat Neurosci. 2011; 14:9–15. [PubMed: 21187849]

Di Marzo V, Fontana A, Cadas H, Schinelli S, Cimino G, Schwartz J-C, Piomelli D. Formation and inactivation of endogenous cannabinoid anandamide in central neurons. 1994

Dowie MJ, Bradshaw HB, Howard ML, Nicholson LFB, Faull RLM, Hannan AJ, Glass M. Altered CB1 receptor and endocannabinoid levels precede motor symptom onset in a transgenic mouse model of Huntington's disease. Neuroscience. 2009; 163:456–465. [PubMed: 19524019]

Engel J Jr, Bragin A, Staba R, Mody I. High-frequency oscillations: What is normal and what is not? Epilepsia. 2009; 50:598–604. [PubMed: 19055491]

Erickson JC, Clegg KE, Palmiter RD. Sensitivity to leptin and susceptibility to seizures of mice lacking neuropeptide Y. Nature. 1996; 381:415–421. [PubMed: 8632796]

Ferraro TN, Golden GT, Smith GG, St Jean P, Schork NJ, Mulholland N, Ballas C, Schill J, Buono RJ, Berrettini WH. Mapping loci for pentylenetetrazol-induced seizure susceptibility in mice. Journal of Neuroscience. 1999; 19:6733–6739. [PubMed: 10436030]

Glass M, Dragunow M, Faull RL. The pattern of neurodegeneration in Huntington“s disease: a comparative study of cannabinoid, dopamine, adenosine and GABA(A) receptor alterations in the human basal ganglia in Huntington”s disease. Neuroscience. 2000; 97:505–519. [PubMed: 10828533]

Glass M, Faull RL, Dragunow M. Loss of cannabinoid receptors in the substantia nigra in Huntington's disease. Neuroscience. 1993; 56:523–527. [PubMed: 8255419]

Horne EA, Coy J, Swinney K, Fung S, Cherry AET, Marrs WR, Naydenov AV, Lin YH, Sun X, Dirk Keene C, et al. Downregulation of cannabinoid receptor 1 from neuropeptide Y interneurons in the basal ganglia of patients with Huntington's disease and mouse models. Eur J Neurosci. 2012; 37 n/a–n/a.

Hsu K-L, Tsuboi K, Adibekian A, Pugh H, Masuda K, Cravatt BF. daGLb inhibition perturbs a lipid network involved in macrophage inflammatory responses. Nat Chem Biol. 2012; 8:999–1007. [PubMed: 23103940]

Hsu K-L, Tsuboi K, Chang JW, Whitby LR, Speers AE, Pugh H, Cravatt BF. Discovery and Optimization of Piperidyl-1,2,3-Triazole Ureas as Potent, Selective, and in Vivo-Active Inhibitors of α/β-Hydrolase Domain Containing 6 (ABHD6). J. Med. Chem. 2013a; 56:8270–8279. [PubMed: 24152295]

Hsu K-L, Tsuboi K, Whitby LR, Speers AE, Pugh H, Inloes J, Cravatt BF. Development and Optimization of Piperidyl-1,2,3-Triazole Ureas as Selective Chemical Probes of Endocannabinoid Biosynthesis. J. Med. Chem. 2013b; 56:8257–8269. [PubMed: 24152245]

Kalume F, Westenbroek RE, Cheah CS, Yu FH, Oakley JC, Scheuer T, Catterall WA. Sudden unexpected death in a mouse model of Dravet syndrome. J. Clin. Invest. 2013; 123:1798–1808. [PubMed: 23524966]

Katona I, Freund TF. Multiple Functions of Endocannabinoid Signaling in the Brain. Annu Rev Neurosci. 2012; 35:529–558. [PubMed: 22524785]

Kwan P, Brodie MJ. Early identification of refractory epilepsy. N Engl J Med. 2000; 342:314–319. [PubMed: 10660394]

Lafourcade M, Elezgarai I, Mato S, Bakiri Y, Grandes P, Manzoni OJ. Molecular components and functions of the endocannabinoid system in mouse prefrontal cortex. PLoS ONE. 2007; 2:e709. [PubMed: 17684555]

Luthi-Carter R, Hanson SA, Strand AD, Bergstrom DA, Chun W, Peters NL, Woods AM, Chan EY, Kooperberg C, Krainc D, et al. Dysregulation of gene expression in the R6/2 model of polyglutamine disease: parallel changes in muscle and brain. Hum Mol Genet. 2002; 11:1911–1926. [PubMed: 12165554]

Luthi-Carter R, Strand A, Peters NL, Solano SM, Hollingsworth ZR, Menon AS, Frey AS, Spektor BS, Penney EB, Schilling G. Decreased expression of striatal signaling genes in a mouse model of Huntington's disease. Hum Mol Genet. 2000; 9:1259–1271. [PubMed: 10814708]

Mangiarini L, Sathasivam K, Seller M, Cozens B, Harper A, Hetherington C, Lawton M, Trottier Y, Lehrach H, Davies SW, et al. Exon 1 of the HD gene with an expanded CAG repeat is sufficient to cause a progressive neurological phenotype in transgenic mice. Cell. 1996; 87:493–506. [PubMed: 8898202]

Marrs WR, Horne EA, Ortega-Gutierrez S, Cisneros JA, Xu C, Lin YH, Muccioli GG, Lopez-Rodriguez ML, Stella N. Dual inhibition of alpha/beta-hydrolase domain 6 and fatty acid amide

hydrolase increases endocannabinoid levels in neurons. Journal of Biological Chemistry. 2011; 286:28723–28728. [PubMed: 21665953]

Marrs WR, Blankman JL, Horne EA, Thomazeau A, Lin YH, Coy J, Bodor AL, Muccioli GG, Hu SS-J, Woodruff G, et al. The serine hydrolase ABHD6 controls the accumulation and efficacy of 2-AG at cannabinoid receptors. Nat Neurosci. 2010; 13:951–957. [PubMed: 20657592]

Marsh DJ, Baraban SC, Hollopeter G, Palmiter RD. Role of the Y5 neuropeptide Y receptor in limbic seizures. Proceedings of the National Academy of Sciences. 1999; 96:13518–13523.

Marsicano G. CB1 Cannabinoid Receptors and On-Demand Defense Against Excitotoxicity. Science. 2003; 302:84–88. [PubMed: 14526074]

Marsicano G, Wotjak CT, Azad SC, Bisogno T, Rammes G, Cascio MG, Hermann H, Tang J, Hofmann C, Zieglgänsberger W, et al. The endogenous cannabinoid system controls extinction of aversive memories. Nature. 2002; 418:530–534. [PubMed: 12152079]

Navia-Paldanius D, Savinainen JR, Laitinen JT. Biochemical and pharmacological characterization of human / -hydrolase domain containing 6 (ABHD6) and 12 (ABHD12). The Journal of Lipid Research. 2012; 53:2413–2424.

Noe F, Pool AH, Nissinen J, Gobbi M, Bland R, Rizzi M, Balducci C, Ferraguti F, Sperk G, During MJ, et al. Neuropeptide Y gene therapy decreases chronic spontaneous seizures in a rat model of temporal lobe epilepsy. Brain. 2008; 131:1506–1515. [PubMed: 18477594]

Nutt DJ, Cowen PJ, Batts CC, Grahame-Smith DG, Green AR. Repeated administration of subconvulsant doses of GABA antagonist drugs. Psychopharmacology. 1982; 76:84–87. [PubMed: 6281839]

Oakley JC, Kalume F, Yu FH, Scheuer T, Catterall WA. Temperature- and age-dependent seizures in a mouse model of severe myoclonic epilepsy in infancy. Proc Natl Acad Sci USA. 2009; 106:3994–3999. [PubMed: 19234123]

Racine RJ. Modification of seizure activity by electrical stimulation. II. Motor seizure. Electroencephalogr Clin Neurophysiol. 1972; 32:281–294. [PubMed: 4110397]

Rudenko V, Rafiuddin A, Leheste JR, Friedman LK. Inverse relationship of cannabimimetic (R+) WIN 55, 212 on behavior and seizure threshold during the juvenile period. Pharmacol Biochem Behav. 2012; 100:474–484. [PubMed: 22019959]

Schindelin J, Arganda-Carreras I, Frise E, Kaynig V, Longair M, Pietzsch T, Preibisch S, Rueden C, Saalfeld S, Schmid B, et al. Fiji: an open-source platform for biological-image analysis. Nat Meth. 2012; 9:676–682.

Schlosburg JE, Blankman JL, Long JZ, Nomura DK, Pan B, Kinsey SG, Nguyen PT, Ramesh D, Booker L, Burston JJ, et al. Chronic monoacylglycerol lipase blockade causes functional antagonism of the endocannabinoid system. Nat Neurosci. 2010; 13:1113–1119. [PubMed: 20729846]

Sigel E, Baur R, Rácz I, Marazzi J, Smart TG, Zimmer A, Gertsch J. The major central endocannabinoid directly acts at GABA(A) receptors. Proc Natl Acad Sci USA. 2011; 108:18150–18155. [PubMed: 22025726]

Smith M, Wilcox KS, White HS. Discovery of antiepileptic drugs. Neurotherapeutics. 2007; 4:12–17. [PubMed: 17199014]

Stella N, Piomelli D. Receptor-dependent formation of endogenous cannabinoids in cortical neurons. Eur J Pharmacol. 2001a; 425:189–196. [PubMed: 11513837]

Stella N, Schweitzer P, Piomelli D. A second endogenous cannabinoid that modulates long-term potentiation. Nature. 1997; 388:773–778. [PubMed: 9285589]

Stella N. Inflammation to Rebuild a Brain: Inflammation in the zebrafish brain stimulates neurogenesis and tissue regeneration. Science. 2012; 338:1303. [PubMed: 23224546]

Thomas G, Betters JL, Lord CC, Brown AL, Marshall S, Ferguson D, Sawyer J, Davis MA, Melchior JT, Blume LC, et al. The Serine Hydrolase ABHD6 Is a Critical Regulator of the Metabolic Syndrome. CellReports. 2013; 5:508–520.

van Rijnsoever C. Requirement of 5-GABAA Receptors for the Development of Tolerance to the Sedative Action of Diazepam in Mice. Journal of Neuroscience. 2004; 24:6785–6790. [PubMed: 15282283]

Vezzani A, Civenni G, Rizzi M, Monno A, Messali S, Samanin R. Brain Res. 1994; Enhanced neuropeptide Y release in the hippocampus is associated with chronic seizure susceptibility in kainic acid treated rats.660:138–143. [PubMed: 7827990]

Vezzani A, Sperk G, Colmers WF. Neuropeptide Y: emerging evidence for a functional role in seizure modulation. Trends Neurosci. 1999; 22:25–30. [PubMed: 10088996]

White HS. Preclinical development of antiepileptic drugs: past, present, and future directions. Epilepsia 44 Suppl. 2003; 7:2–8.

Wilson RI, Nicoll RA. Endogenous cannabinoids mediate retrograde signalling at hippocampal synapses. Nature. 2001; 410:588–592. [PubMed: 11279497]

Woldbye DP, Larsen PJ, Mikkelsen JD, Klemp K, Madsen TM, Bolwig TG. Powerful inhibition of kainic acid seizures by neuropeptide Y via Y5-like receptors. Nat Med. 1997; 3:761–764. [PubMed: 9212103]

Woldbye DP, Madsen TM, Larsen PJ, Mikkelsen JD, Bolwig TG. Neuropeptide Y inhibits hippocampal seizures and wet dog shakes. Brain Res. 1996; 737:162–168. [PubMed: 8930362]

Zhang X, Bertaso F, Yoo JW, Baumgärtel K, Clancy SM, Van Lee, Cienfuegos C, Wilmot C, Avis J, Hunyh T, et al. Deletion of the potassium channel Kv12.2 causes hippocampal hyperexcitability and epilepsy. Nature Publishing Group. 2010; 13:1056–1058.

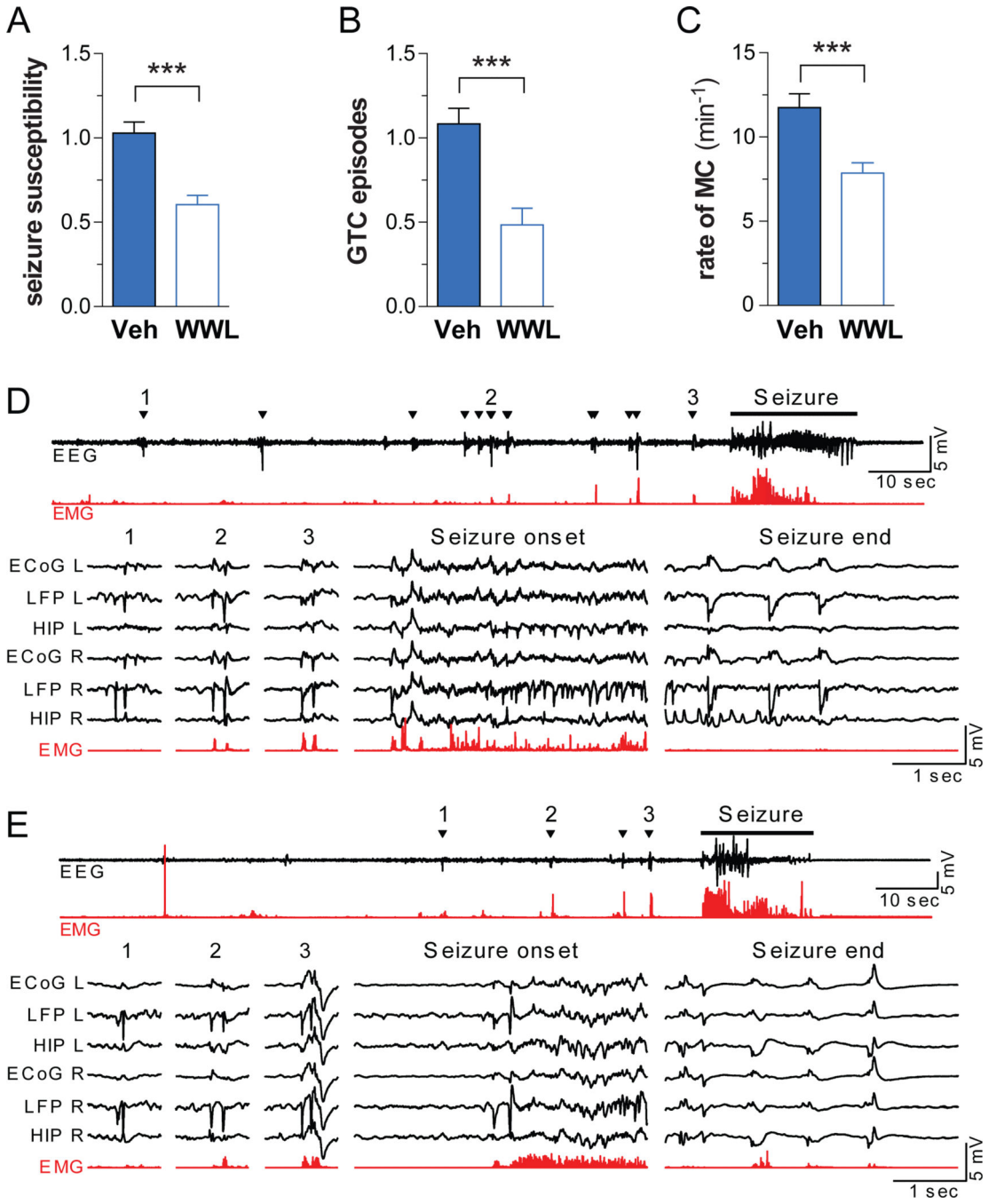

Figure 1. ABHD6 blockade decreases PTZ-induced seizure incidence and severity

(A) Mice pretreated with WWL123 (n=33) experienced less severe PTZ-induced seizures (as calculated by the latencies to Stage 2-4, see methods), (B) fewer global tonic-clonic (GTC) seizures, and (C) fewer myoclonic (MC) seizures, compared to mice pretreated with vehicle (n=37). Results represent pooled data from all experiments performed on C57BL/6 males in this study. One week after surgical electrode implantation, mice were treated with (D) PTZ or (E) PTZ+WWL and EEG measurements were recorded. Condensed EEG (black) with corresponding EMG (red) is presented at the top, and 3 myoclonic seizures, along with

the onset and end of the GTC seizures, are presented in greater detail below. Myoclonic seizures were accompanied by behavioral myoclonus (triangles). Fewer myoclonic seizures were observed in mice pretreated with WWL123. GTC seizures observed in mice receiving either PTZ or PTZ+WWL were similar in nature. Fisher's T-Test was used for post-hoc analyses with *$P<0.05$, **$P<0.01$, ***$P<0.001$. Error bars show SEM.

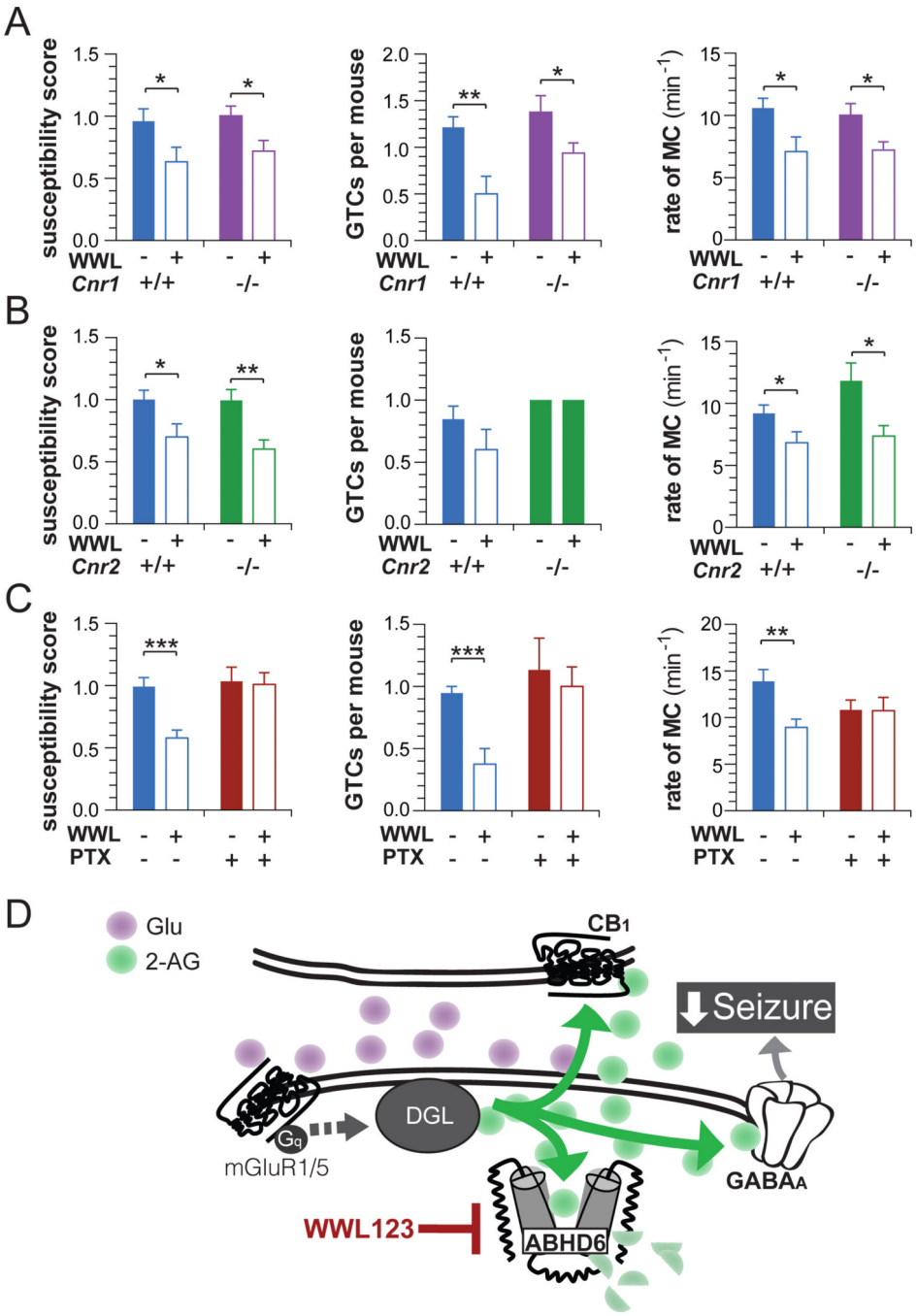

Figure 2. The antiepileptic effect of ABHD6 inhibition is independent of cannabinoid receptors and is blocked by $GABA_A$ antagonism

(A) WT (veh: n=13, WWL123 n=7) and *cnr1*$^{-/-}$ mice (veh, n=16; WWL123, n=17) were pretreated with vehicle or WWL123, and then seizures were induced by PTZ. The antiepileptic effect of WWL123 was intact in *cnr1*$^{-/-}$ mice as measured by seizure susceptibility, number of GTCs and rate of MC. (B) WT (veh, n=13; WWL, n=10) and *cnr2*$^{-/-}$ mice (veh, n=10; WWL123, n= 9) were pretreated with vehicle or WWL123, and seizures were induced by PTZ. WWL123 reduced seizure susceptibility, and MC, but failed

to reduce GTCs in either WT or *cnr2*$^{-/-}$ mice. (C) WT mice were pretreated with vehicle/vehicle (n=19), WWL123/vehicle (n=16), vehicle/picrotoxin (n=15), or WWL123/picrotoxin (n=16), and then seizures were induced by PTZ. The antiepileptic effect of WWL123 was abolished by picrotoxin in all three measures. (D) Proposed mechanism: ABHD6 blockade increases synaptic concentration of 2-AG, resulting in increased activation of $GABA_A$ receptors which exerts antiepileptic effects. Fisher's T-Test was used for post-hoc analyses with **P*<0.05, ***P*<0.01, ****P*<0.001. Error bars show SEM.

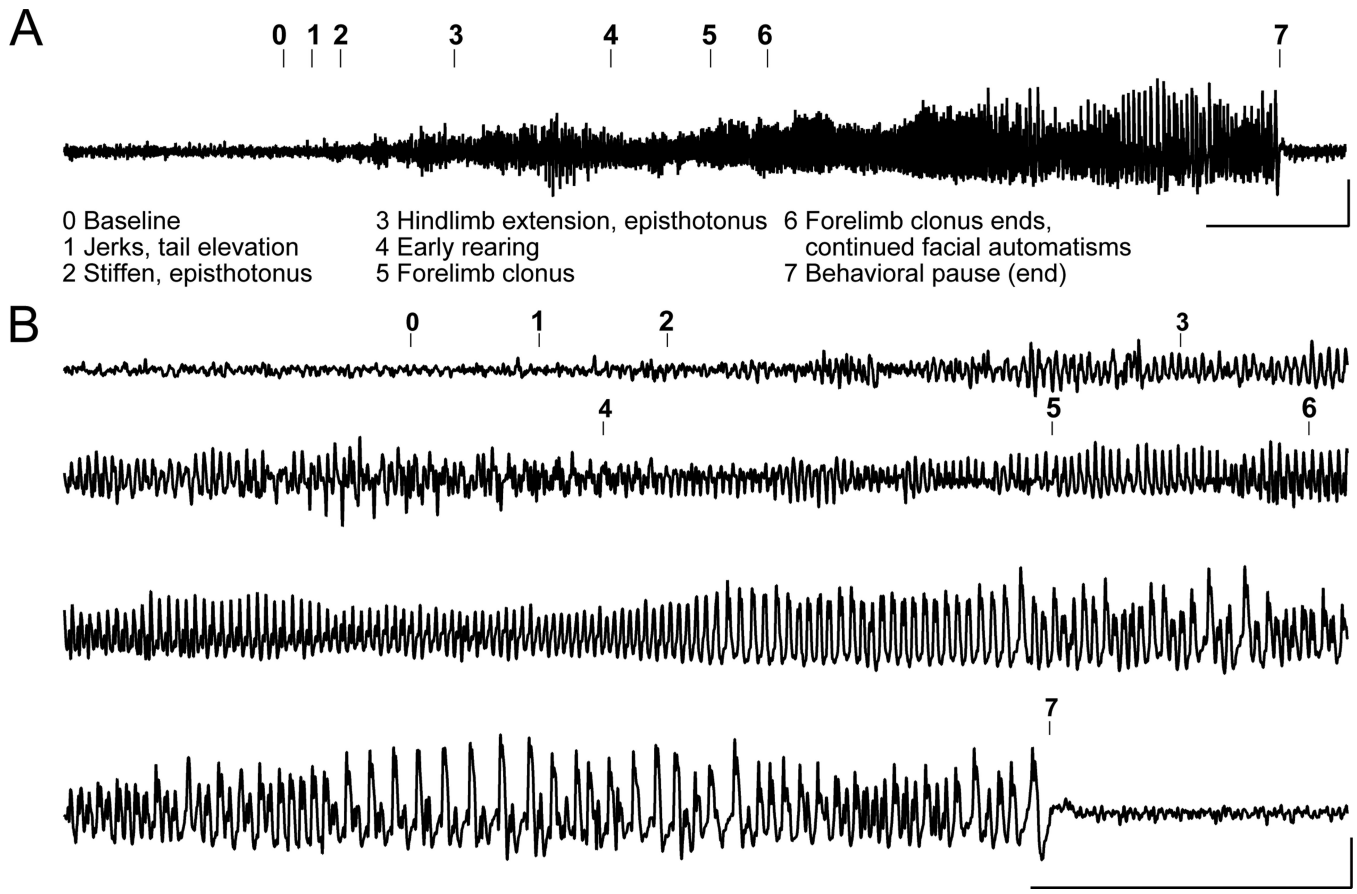

Figure 3. R6/2 mice experience spontaneous electrographic seizures with corresponding seizure behaviors

(A) Representative compressed electroencephalogram from cortical lead depicting a spontaneous electrographic seizure in an R6/2 mouse, with seizure behaviors identified at the time of occurrence (numbers). Background EEG is shown before seizure onset, evolves into rhythmic, sharply contoured spikes, and resolves with clear postictal suppression accompanied by a behavioral pause; calibrator depicts 0.0005V, 20s. (B) Time expanded EEG recording calibrator depicts 5s, 0.0005V.

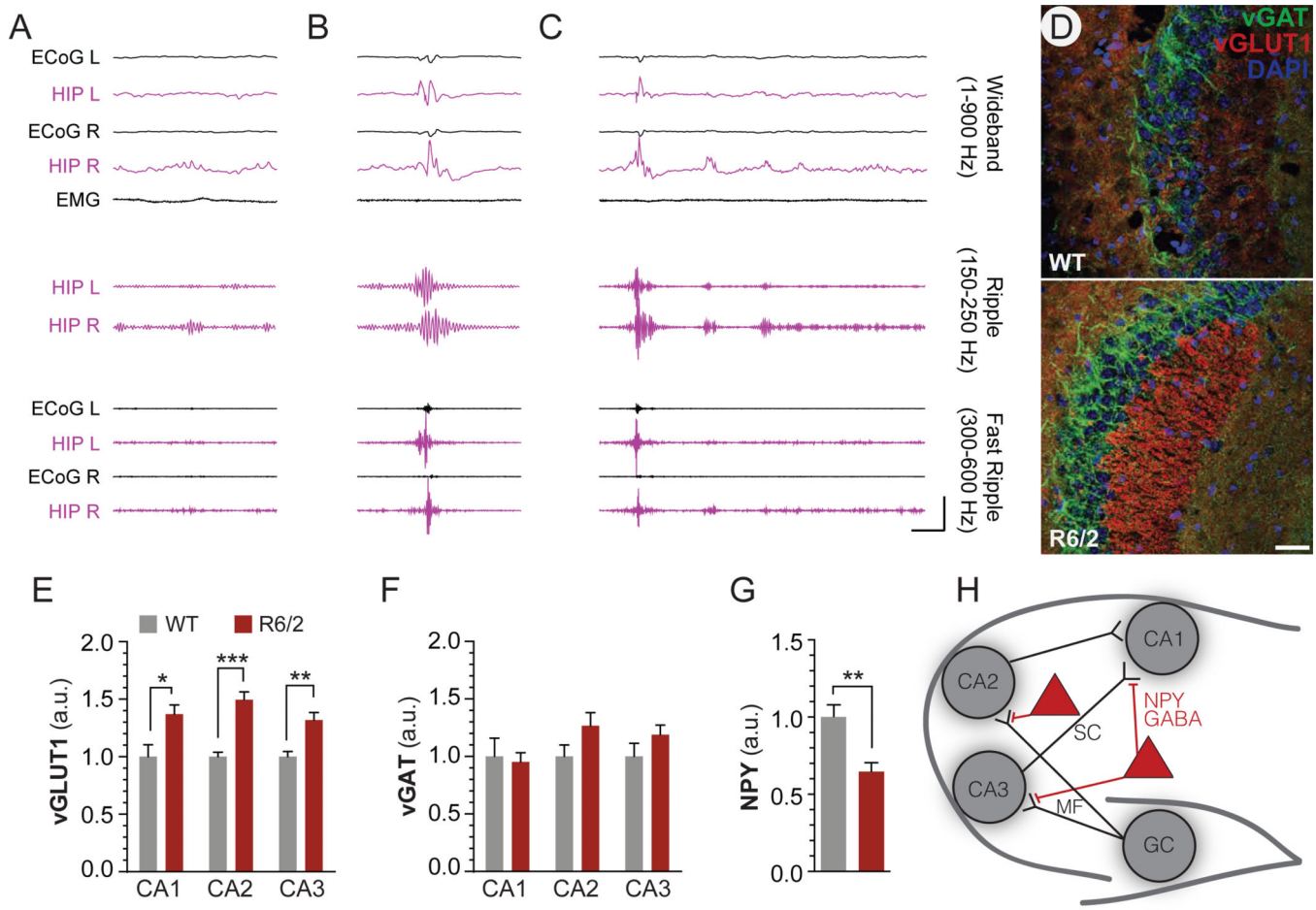

Figure 4. Electrographic and histological abnormalities in the hippocampus of R6/2 mice

Representative example of hippocampal theta/gamma oscillations (A) and two representative examples of interictal discharges in R6/2 mice (B-C). Calibrator depicts 100ms, 5mV (wideband) or 0.5mV (ripple and fast ripple). Discharges in R6/2 mice exceeded 3mV in hippocampal leads (maximal voltage: B= 4.5mV, C= 5.0mV), a common criterion for epileptic discharge, and featured higher amplitude in ripple components (maximal peak-to-peak amplitude: A = 202μV; B = 587μV; C = 904μV) as well as a fast ripple component not observed in theta/gamma (maximal peak-to-peak amplitude: B = 876μV, C= 847μV). (D) Representative 20X images of vGLUT1 and vGAT staining in CA2 depict increased intensity of vGLUT1 staining in the stratum lucidum of R6/2 mice. Increased in vGLUT1 immunoreactivity (E) which was best observed in the stratum lucidum of CA2, but also measureable in CA1 and CA3, and which was not accompanied by an increase in vGAT immunoreactivity (F). (G) Loss of NPY immunoreactivity is detected throughout the hippocampus in R6/2 mice (for details see Figure S6). (H) Model depicting the NPY component of the hippocampal circuit; NPY interneurons provide presynaptic inhibition of mossy fiber (MF) and Schaffer collateral (SC) fibers, and reduction of this inhibition is associated with increased excitatory signaling. Measurements were made after thresholding to mean+SD (vGLUT1 and vGAT), or mean+2*SD (NPY), as determined by the percent of pixels for each stain which represented staining of target proteins. Scale bar

depicts 50μm. Error bars show SEM, and Fisher's T-test is indicated as *$P<0.05$, **$P<.01$, ***$P<.001$.

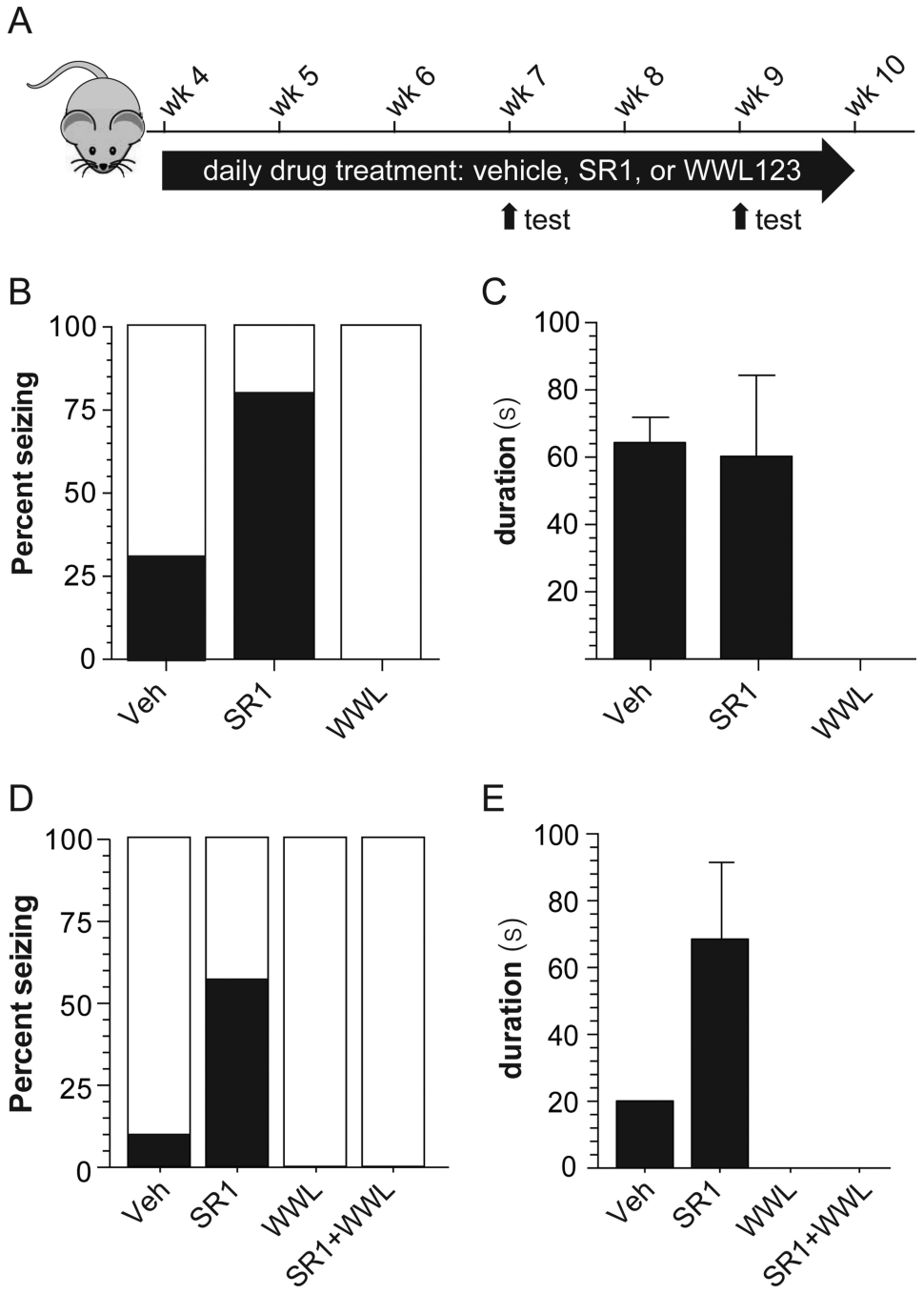

Figure 5. ABHD6 blockade blocks spontaneous behavioral seizures in R6/2 mice in a CB_1-independent manner

(A) R6/2 mice were treated with WWL123, SR141716 (SR1), or vehicle daily starting at 4 weeks of age. Six hour video-recorded seizure observations were performed after the daily drug treatment at 7 weeks and 9 weeks of age, and the data were pooled in order to obtain a more accurate estimate of seizure incidence using multiple observations. Seizure incidence was measured by scoring seizure behaviors corresponding to Racine 4-6 for i.p. vehicle (n=6), s.c. vehicle (n=6), 10 mg/kg i.p. WWL123 (n=5), and 10 mg/kg s.c. SR1 (n=5); the two vehicle groups did not differ from each other and were thus pooled for analysis. (B) SR1

treatment increased seizure incidence relative to vehicle treatment, and WWL123 treatment abolished seizures. (C) Seizure duration was unchanged between vehicle and SR1-treated mice under this chronic treatment regimen. In order to assess mechanism of action, drug-naïve R6/2 mice were treated acutely with vehicle (n=12), SR1 (n=8), WWL123 (n=8), or SR1+WWL123 (n=8), and seizure incidence was scored during the single six hour observation. (D) Acute SR1 treatment increased seizure incidence relative to acute vehicle treatment, and acute WWL123 treatment abolished all seizures, even in mice co-treated with SR1. (E) Seizure duration was not statistically tested because only one seizure was captured in the vehicle group (Veh=20s; SR1=51±34s). Error bars show SEM.